



Case Report

Impact on bone microarchitecture and failure load in a patient with type I Gaucher disease who switched from Imiglucerase to Eliglustat

Karamjot Sidhu^{a,b}, Steven K. Boyd^a, Aneal Khan^{b,c,*}^a McCaig Institute for Bone and Joint Health, Cumming School of Medicine, University of Calgary, 3280 Hospital Drive NW, Calgary, Alberta T2N 4Z6, Canada^b Alberta Children's Hospital Research Institute, Cumming School of Medicine, University of Calgary, 28 Oki Drive NW, Calgary, Alberta T3B 6A8, Canada^c Medical Genetics and Pediatrics, Cumming School of Medicine, University of Calgary, 28 Oki Drive NW, Calgary, Alberta T3B 6A8, Canada

ARTICLE INFO

Keywords:

Gaucher disease

Bone disease

High-resolution peripheral quantitative computed tomography

Finite element analysis

Enzyme replacement therapy

Substrate replacement therapy

ABSTRACT

Gaucher disease (GD; OMIM 230800) is a lysosomal storage disorder caused by a deficiency in acid beta-glucosidase as a result of mutation in the *GBA* gene. Type 1 GD (GD1) is the most common form and its clinical manifestations include severe hematological, visceral and bone disease. The goal of disease-modifying treatments for GD1 is to reduce substrate storage and hence toxicity from the disease. The two common therapeutic routes for managing GD1 are enzyme replacement therapy (ERT) and substrate reduction therapy (SRT). These therapies have shown to improve hematological and visceral aspects of the disease. However, quantitative investigations into how these therapies may help prevent or improve the progression of bone disease is limited. This case involves a patient diagnosed with GD1 in childhood, who began ERT in young adulthood. Following over 20 years of treatment with ERT, the patient switched to SRT. This case report examined the novel application of high-resolution peripheral quantitative computed tomography (HR-pQCT) in a patient who switched from ERT to SRT. Using bone microarchitecture measurements from HR-pQCT, we applied finite element analysis techniques to calculate the failure load which estimates the resistance to fracture. Over the course of one year following the switch from ERT to SRT therapy, failure load improved in the patient's lower limb. In conclusion, failure load can be computed in the short term in a patient who made a switch from ERT to SRT. Further exploration of failure load in study design to look at interventions that impact bone quality in GD may be considered.

1. Introduction

Gaucher disease (GD) is an inherited disorder caused by a deficiency of enzyme acid-beta-glucosidase (EC 3.2.1.45). With type 1 GD (GD1; OMIM 230800), the most common form of GD, 94% of all patients registered on the International Collaborative Gaucher Group (ICGG) registry showed radiological evidence of some degree of bone involvement [1]. Some of the common bone complications that have been reported include osteopenia, marrow infiltration, avascular necrosis, and fractures [1]. Infiltration of bone marrow tissue by Gaucher cells, splenectomy, anemia, and impaired mobility are some of the common causes proposed to motivate these complications [1–3].

To date, studies investigating the longitudinal effects of therapies on bone quality have been dominated by qualitative and semiquantitative measures, such as recording patient/clinician-reported bone crises,

radiographic findings and MRI-derived bone marrow burden score [4,5]. Quantitative studies examining skeletal changes longitudinally have been strictly limited to areal bone mineral density (BMD) assessed by dual-energy X-ray absorptiometry (DXA). However, a shortcoming of DXA is its inability to detect change in BMD within short time intervals, and large changes in BMD are often required before being captured on DXA [6]. Previous studies that have examined therapeutic treatment effect on skeletal status have demonstrated significant improvement in DXA-assessed BMD over the course of multiple years [7]. Moreover, relying solely on BMD has shown to be inadequate in monitoring bone disease in GD patients, rather factors such as bone microarchitecture and geometry all play a crucial role in fracture risk assessment and warrant further investigation in monitoring bone involvement in these patients [8].

High-resolution peripheral quantitative computed tomography (HR-

Abbreviations: GD, Gaucher Disease; GD1, Gaucher Disease (type I); ICGG, International Collaborative Gaucher Group; DXA, Dual-energy x-ray absorptiometry; HR-pQCT, High-resolution peripheral quantitative computed tomography; MRI, Magnetic resonance imaging; BMD, Bone mineral density; ERT, Enzyme replacement therapy; SRT, Substrate reduction therapy; LS, Lumbar spine; FN, Femoral neck; LSC, Least significant change

* Corresponding author at: Medical Genetics and Pediatrics, University of Calgary, Alberta Children's Hospital, 28 Oki Drive NW, Calgary, Alberta T3B 6A8, Canada.

E-mail addresses: kksidhu@ucalgary.ca (K. Sidhu), skboyd@ucalgary.ca (S.K. Boyd), khaa@ucalgary.ca (A. Khan).

<https://doi.org/10.1016/j.ymgmr.2020.100606>

Received 26 February 2020; Received in revised form 9 May 2020; Accepted 10 May 2020

2214-4269/© 2020 The Authors. Published by Elsevier Inc. This is an open access article under the CC BY-NC-ND license (<http://creativecommons.org/licenses/by-nc-nd/4.0/>).

pQCT), is non-invasive, in vivo bone imaging modality, that images bone at the distal radius and distal tibia, providing a volumetric measurement of BMD and three-dimensional assessment of bone microarchitecture. This novel technique has the ability to examine important and fracture-relevant structural properties of cortical and trabecular bone independently and has demonstrated higher sensitivity in detecting changes in skeletal status when compared to DXA [6]. HR-pQCT also offers the possibility of predicting bone strength by measuring failure load using finite element techniques. The finite element method is a computational approach that performs biomechanical simulations on HR-pQCT bone scan data, such as compressive loading, and has shown strong correlation with mechanical testing on cadaveric material [9]. Predicted failure load from these simulations has also shown to provide valuable information about skeletal fragility and enhance fracture prediction [10]. These methods offer the possibility to provide a more personalized assessment of fracture risk as the individual's own bone scan data is used to calculate failure load, a better application to GD where there is high inter-variability. This is the first case report using the application of HR-pQCT and finite element methods to compute failure load in a patient with GD1 while on ERT and after switching to SRT.

2. Materials and methods

This case report is on a 39-year-old male patient who was diagnosed with GD1 at 5 years of age with a presentation of bone pain but no evidence of ischemic bone disease or fracture on magnetic resonance imaging (MRI). Genetic testing revealed compound heterozygous mutations for N370S (c.1226A > G; p.Asn409Ser) and G377S (c.1246G > A; p.Gly416Ser). During the time of the study he was on standard clinical management. Once referred to a treatment centre, ERT (imiglucerase, Sanofi Genzyme®, Massachusetts, United States) was started at 18 years of age with initial approval for 20 mg/kg biweekly. After 37 years of age, a dose of 30 mg/kg biweekly was approved and started. However, at 30 years of age, ERT was interrupted because of a global imiglucerase shortage. From age 38-years-old, he began SRT (84 mg twice daily of eliglustat, Sanofi Genzyme®, Massachusetts, United States). The decision to switch treatments was patient-initiated and standard care was followed. The patient was advised to supplement his diet with vitamin D (3000 IU daily). Patient had no history of bisphosphonate use. Previous musculoskeletal complications include a traumatic metatarsal fracture and sport-related tear of the Achilles tendon.

As per standard clinical care, laboratory parameters were monitored. Standard tests were performed in local laboratories (Alberta Public Laboratories, Alberta, Canada) and chitotriosidase, angiotensin converting enzyme, and tartrate resistance acid phosphatase were sent to Sanofi Genzyme® Laboratories (Massachusetts, United States).

In accordance to standard care, areal BMD of lumbar spine (LS) and femoral neck (FN) were measured using DXA (Hologic QDR 4500 W®, Hologic Inc., Bedford, United States). In addition to standard care, HR-pQCT scans of the distal radius and distal tibia were captured

(XtremeCT®, Scanco Medical, Bruttisellen, Switzerland). The effective radiation dose using HR-pQCT is approximately 5 µSv per scan [11]. For comparison, a hip or spine DXA scan result in an average effective radiation dose of 9 to 13 µSv per scan, respectively [12]. All scans underwent assessment for quality related to movement artifact and were graded on a scale of 1 (little or no motion) to 5 (severe blurring and discontinuities) [13]. Scans with a score of 4 or higher were not analyzed. Density values measured from HR-pQCT scan data included total BMD (mg HA/cm³), cortical BMD (mg HA/cm³), and trabecular BMD (mg HA/cm³). For microarchitecture, trabecular number (mm⁻¹) and cortical thickness (mm) were examined. All parameters from HR-pQCT bone scans were derived from the largest common region amongst all scans.

To calculate failure load, finite element analysis was performed on unmatched images and required a largest common region of at least 90% [14]. Serial measurements with a common region less than 90% are at risk for findings associated with change in the region of bone under investigation. A voxel-conversion approach was used to generate linear, homogenous finite element meshes from HR-pQCT image data [15,16]. The finite element analysis protocol employed has been described in detail, previously [10]. The measured outcome from finite element analysis was failure load in Newtons (N). All HR-pQCT and failure load measurements were compared to healthy age- and sex-matched controls [17].

Least significant change (LSC), a statistical calculation recommended by the International Society for Clinical Densitometry, was calculated for DXA- and HR-pQCT-measured density and HR-pQCT-measured microarchitecture to objectively evaluate whether the observed change was outside the range of measurement error [14]. The LSC for male radius was: total BMD (1.8%), cortical BMD (0.9%), trabecular BMD (1.9%), cortical thickness (4.0%), trabecular number (9.8%). The LSC for male tibia was: total BMD (1.5%), cortical BMD (0.8%), trabecular BMD (1.5%), cortical thickness (2.5%), trabecular number (8.7%). For DXA, the manufacturer-reported LSC for the Hologic DXA was used as DXA scans were performed at various medical facilities. The LSC reported for LS-BMD and FN-BMD was 3.0% and 4.2%, respectively [18].

3. Results

The patient demonstrated well-controlled hematologic parameters and visceral manifestations and maintained a normal and stable peripheral white blood cell count, platelet count and hemoglobin levels. Minimum and maximum values of standard and GD-specific biomarkers measured during the investigation are presented as a range in Table 1. A 595 nmol/h/mL increase in chitotriosidase resulted due to a brief cessation of treatment because of a global imiglucerase shortage. The patient continued to have occasional mild bone pain in the hip, spine and hands but was negative on MRI for surveillance of ischemic bone disease or fractures and the pain was not significant enough for him to consider analgesics or reduction in activities. Clinical examination remained normal during the observation period with the exception of

Table 1
Minimum and maximum measurements from standard and GD-specific serum tests during the investigation.

	Serum Test	Patient's Results	Reference Range
Standard biomarkers	Hemoglobin	141–153 g/L	130–170 g/L
	Platelets	180–222 10 ⁹ /L	150–400 10 ⁹ /L
	White blood cell count	5.2–6.5 10 ⁹ /L	4.0–11.0 10 ⁹ /L
GD-Specific biomarkers	Chitotriosidase	96–595 [#] nmol/h/mL	4–120 nmol/h/mL
	Angiotensin-converting enzyme	61–65 IU/L	25–106 IU/L
	Tartrate-resistant acid phosphatase	5.5–7.8 IU/L	3–10 IU/L

[#]The patient experienced a 595 nmol/h/mL increase in chitotriosidase due to a brief cessation of treatment because of a global shortage of imiglucerase. This increase in chitotriosidase was captured at 30 years of age, and the following measurement was taken at 32 years of age where chitotriosidase returned to 163 nmol/h/mL.

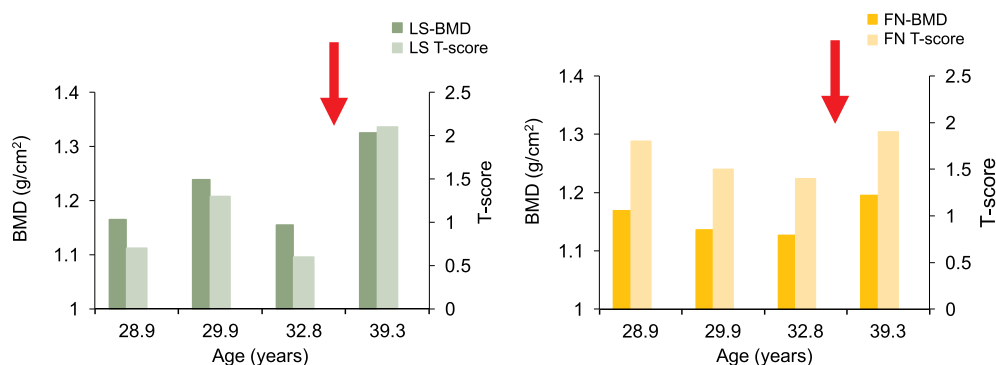


Fig. 1. (Left) Patient's LS-BMD and LS T-score. (Right) Patient's FN-BMD and LS T-score. Red arrow represents the switch from imiglucerase to eliglustat therapy.

mild hepatosplenomegaly. No hospitalization and no bone crises occurred during the investigation.

3.1. Findings from DXA

Fig. 1 illustrates changes in DXA scores. While on imiglucerase, LS-BMD experienced an increase followed by a decrease similar in magnitude, $+0.6 \text{ g/cm}^2$ and -0.7 g/cm^2 , respectively. Following cessation of imiglucerase and initiation of eliglustat, LS-BMD increased by 14.7% (1.155 to 1.325 g/mm^2), and the LS T-score increased from 0.6 to 2.1. These changes observed in LS-BMD were above the LSC. At the hip, FN-BMD remained stable while on imiglucerase and changes observed in FN-BMD were below the LSC. Following initiation of eliglustat treatment, FN-BMD increased by 6.0% from the previous measurement while on imiglucerase (1.127 to 1.195 g/cm^2), and this change was above the LSC. This was accompanied by an increase in the FN T-score (1.4 to 1.9). Both LS and FN T-scores remained well above the range defined as low bone mass (previously known as osteopenia) and osteoporotic T-scores (-1.0 to -2.5 and less than -2.5 , respectively) [19].

3.2. Findings from HR-pQCT & finite element analysis

HR-pQCT findings show total BMD, trabecular BMD, and trabecular number in the upper limbs remained stable while on imiglucerase treatment and one year following the switch to eliglustat treatment. Whereas cortical BMD in the upper limb, increased while on imiglucerase treatment ($+1.61\%$, $+14.5 \text{ mg HA/mm}^3$) but remained stable while on eliglustat. Similarly, cortical thickness increased during imiglucerase treatment ($+2.83\%$, $+0.03 \text{ mm}$) and this cortical thickness is maintained one year following eliglustat treatment. In the lower limb, cortical BMD, trabecular BMD, and trabecular number remained stable. Total BMD increased while on imiglucerase treatment ($+1.28\%$, $+5.3 \text{ mg HA/mm}^3$) and remained stable while on eliglustat treatment. Cortical thickness in the tibia experienced an increase while on imiglucerase treatment ($+4.03\%$, $+0.08 \text{ mm}$), and increased one year after switching to eliglustat treatment ($+4.18\%$, $+0.09 \text{ mm}$). The total BMD in the patient remained above the 85th %ile in both the upper and lower limbs while on imiglucerase treatment and one year following eliglustat treatment when compared to age- and sex-matched controls.

For the radius and tibia, 76% and 97% of the 104 slices were common amongst the scans, respectively. Given the largest common region amongst the serial measurements of the radius was below 90%, they were excluded from finite element analysis. The failure load of the tibia HR-pQCT scan revealed a steady increase while on imiglucerase over the course of three years ($+2.22\%$, 204.9 N ; Fig. 2). Failure load also increased following treatment with eliglustat ($+2.43\%$, 228.5 N).

4. Discussion

Fractures can often be the most debilitating aspect of GD1 and can significantly impact quality of life [20]. However, in large clinical trials, quantitative examinations of bone have been neglected as bone's response to treatments is more difficult to capture and often lags behind in comparison to hematologic parameters and visceral disease. In this case report, we applied HR-pQCT imaging of the distal limb bones in the course of therapy of a patient with Gaucher disease. Failure load was computed from the HR-pQCT bone scan data to estimate bone strength. During the course of period observation, the patient underwent a switch from imiglucerase to eliglustat. Failure load improved while on imiglucerase therapy and one year following the switch from imiglucerase to eliglustat. Alongside the improvement in failure load, cortical thickness increased while in imiglucerase treatment, and one year following the switch to eliglustat treatment.

Following over 20 years of treatment with imiglucerase, BMD at the spine and hip remained stable. After switching to eliglustat, the BMD of the spine and hip both experienced an increase despite being in the non-osteopenic range initially. The largest changes were witnessed in the BMD and T-score of the lower spine, whereas the hip experienced a smaller change. This pattern is relevant to GD patients since most fractures occur in the lower spine [2] compared to the general population where they occur mostly in the hip [21]. Findings from HR-pQCT indicated both density and microarchitecture were stable, with the exception of cortical thickness, which increased while on imiglucerase therapy, and one year after switching to eliglustat. Previous literature has demonstrated cortical thickness plays a crucial role in fracture assessment [22,23]. The patient's cortical thickness percentile ranking when compared to healthy age- and sex-matched controls was considerably higher in the lower limbs when compared to the upper limbs (91st versus 71th, respectively). This highlights the importance of weight-bearing while on treatment to ensure the most optimal outcome.

The current standard imaging modality for assessing fracture risk, DXA, can only explain part of the variation in bone strength [24]. This is in part due to the fact that DXA uses areal density as a surrogate for bone strength whereas strength is estimated directly by computing failure load from the three-dimensional HR-pQCT bone scan, which intrinsically includes volumetric density and microarchitectural characteristics. Estimated bone strength predicted from failure load for the lower limb improved over the course of treatment with imiglucerase, and after switching to eliglustat. The overall trend of the patient's failure load was observed to be in the upward direction when compared to the percentile curves for healthy age- and sex-matched controls. This is relevant because it showcases that treatment for the Gaucher disease, without the use of bone-modifying therapies (i.e. bisphosphonates, parathyroid hormone), played an important role in combatting the accelerated bone loss that was to occur from the GD diagnosis in addition to age-related bone loss. The failure load assessed at the distal tibia in males has been shown to have strong correlation with failure

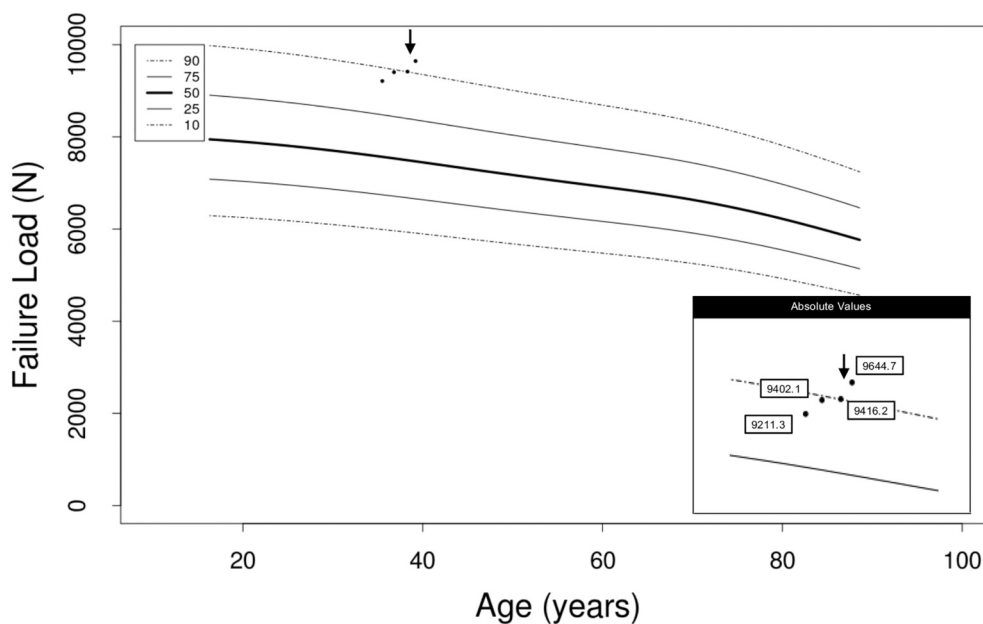


Fig. 2. Patient's failure load results from compressional testing of the distal tibia. Arrow represents the switch from imiglucerase to eliglustat therapy. Lines represent percentile curves (top-to-bottom: 90th, 75th, 50th, 25th, 10th). Absolute values reported in Newtons (N). Percentile curves generated on www.Normative.ca [17].

load at common axial osteoporotic sites, spine and hip ($r = 0.90$ and $r = 0.83$, respectively) [25]. Furthermore, findings from the Osteoporotic Fractures in Men (MrOS) study [26] reported a lower failure load was an independent predictor of osteoporotic and clinical fractures.

This case report demonstrated long-term use of ERT, followed by a switch to SRT played a role in preventing or delaying accelerated bone loss in this patient. In conclusion, we found that bone microarchitecture and bone strength can be computed in the short term in a patient who made a switch from ERT to SRT using HR-pQCT and finite element methods. Further exploration of this technology may be considered as part of study designs to look at interventions that impact bone quality in GD.

Contributions of individual authors

Karamjot Sidhu helped with data curation and analysis, and constructed the manuscript.

Steven Boyd helped design the observational plan and data analysis.

Aneal Khan helped design the observational plan and data curation and was responsible for clinical patient care and diagnostics.

All authors reviewed and edited the manuscript.

Funding

This research did not receive any specific grant from funding agencies in the public, commercial, or not-for-profit sectors.

Details of ethics approval

This study was carried out in accordance with the ethical standard of the responsible committee on human experimentation, The Code of Ethics of the World Medical Association (Declaration of Helsinki). The University of Calgary's Conjoint Health Research Ethics Board (CHREB) approved this study (REB#15-0271).

Availability of data and material statement

Raw data from high-resolution peripheral quantitative computed tomography (HR-pQCT) will be provided upon request for 25 years

following publication date. After which the data will be destroyed as per institutional guidelines for data management. All other data has been provided directly in the manuscript.

Declaration of Competing Interest

Aneal Khan has received speaker honorarium, travel grants, and consultation fees from Genzyme Corporation® (a Sanofi® Company) and is a member of the International Collaborative Gaucher Group (ICGG). Karamjot Sidhu and Steven Boyd have declared no conflict of interest.

Acknowledgements

The authors wish to thank the patient for sharing his clinical data, as well as the staff of Alberta Children's Hospital and McCaig Institute for Bone and Joint Health for booking appointments and collecting the imaging data, including Karin Klassen, Sheryl Jackson, Karen Sabo, Shelly Carle, and Alice Li.

References

- [1] J. Charrow, H.C. Andersson, P. Kaplan, E.H. Kolodny, P. Mistry, G. Pastores, et al., The Gaucher registry: demographics and disease characteristics of 1698 patients with Gaucher disease, *Arch. Intern. Med.* 160 (18) (2000) 2835–2843.
- [2] A. Khan, T. Hangartner, N.J. Weinreb, J.S. Taylor, P.K. Mistry, Risk factors for fractures and avascular osteonecrosis in type 1 Gaucher disease: a study from the international collaborative Gaucher group (ICGG) Gaucher registry, *J. Bone Miner. Res.* 27 (8) (2012) 1839–1848.
- [3] R.J. Wenstrup, M. Roca-Espiau, N.J. Weinreb, B. Bemb, Skeletal aspects of Gaucher disease: a review, *Br. J. Radiol.* 75 (2002) A2–A12.
- [4] P.L. Robertson, M. Maas, J. Goldblatt, Semiquantitative assessment of skeletal response to enzyme replacement therapy for Gaucher's disease using the bone marrow burden score, *Am. J. Roentgenol.* 188 (6) (2007) 1521–1528.
- [5] N.J. Weinreb, J. Charrow, H.C. Andersson, P. Kaplan, E.H. Kolodny, P. Mistry, et al., Effectiveness of enzyme replacement therapy in 1028 patients with type 1 Gaucher disease after 2 to 5 years of treatment: a report from the Gaucher registry, *Am. J. Med.* 113 (2) (2002) 112–119.
- [6] K.K. Nishiyama, H.M. Macdonald, D.A. Hanley, S.K. Boyd, Women with previous fragility fractures can be classified based on bone microarchitecture and finite element analysis measured with HR-pQCT, *Osteoporos. Int.* 24 (5) (2013) 1733–1740.
- [7] R.S. Kamath, E. Lukina, N. Watman, M. Dragosky, G.M. Pastores, et al., Skeletal improvement in patients with Gaucher disease type 1: a phase 2 trial of oral eliglustat, *Skelet. Radiol.* 43 (10) (2014) 1353–1360.
- [8] M. Baldini, G. Casirati, F.M. Olivieri, E. Cassinerio, K.K. Chalouhi, E. Poggiali, et al.,

- Skeletal involvement in type 1 Gaucher disease: Not just bone mineral density, *Blood Cells Mol. Dis.* 68 (2018) 148–152.
- [9] J.A. MacNeil, S.K. Boyd, Bone strength at the distal radius can be estimated from high-resolution peripheral quantitative computed tomography and the finite element method, *Bone*. 42 (6) (2008) 1203–1213.
- [10] S. Boutroy, B. van Rietbergen, E. Sornay-Rendu, F. Munoz, M.L. Bouxsein, P.D. Delmas, Finite element analysis based on in vivo HR-pQCT images of the distal radius is associated with wrist fracture in postmenopausal women, *J. Bone Miner. Res.* 23 (3) (2008) 392–399.
- [11] K.K. Nishiyama, E. Shane, Clinical imaging of bone microarchitecture with HR-pQCT, *Curr. Osteoporos. Rep.* 11 (2) (2013) 147–155.
- [12] J. Damilakis, J.E. Adams, G. Guglielmi, T.M. Link, Radiation exposure in X-ray-based imaging techniques used in osteoporosis, *Eur. Radiol.* 20 (11) (2010) 2707–2714.
- [13] Y. Pauchard, A.M. Liphardt, H.M. Macdonald, D.A. Hanley, S.K. Boyd, Quality control for bone quality parameters affected by subject motion in high-resolution peripheral quantitative computed tomography, *Bone*. 50 (6) (2012) 1304–1310.
- [14] J.A. MacNeil, S.K. Boyd, Improved reproducibility of high-resolution peripheral quantitative computed tomography for measurement of bone quality, *Med. Eng. Phys.* 30 (6) (2008) 792–799.
- [15] R. Müller, P. Rüeeggsegger, Three-dimensional finite element modelling of non-invasively assessed trabecular bone structures, *Med. Eng. Phys.* 17 (2) (1995) 126–133.
- [16] B. van Rietbergen, H. Weinans, R. Huiskes, A. Odgaard, A new method to determine trabecular bone elastic properties and loading using micromechanical finite-element models, *J. Biomech.* 28 (1) (1995) 69–81.
- [17] L.A. Burt, Z. Liang, T.T. Sajobi, D.A. Hanley, S.K. Boyd, Sex-and site-specific normative data curves for HR-pQct, *J. Bone Miner. Res.* 31 (11) (2016) 2041–2047.
- [18] K.E. Wilson, A.P. Smith, Monitoring BMD with DXA: Short-and Long-term Precision, <https://pdfs.semanticscholar.org/1741/be4d21b4a9f2afbc5b5ad2dfd9d91c63256b.pdf>, (2009) , Accessed date: 21 November 2019.
- [19] World Health Organization, Assessment of fracture risk and its application to screening for postmenopausal osteoporosis: report of a WHO study group, *World Health Organ. Tech. Rep. Ser.* 843 (1994) 1–129.
- [20] N. Weinreb, J. Barranger, S. Packman, A. Prakash-Cheng, B. Rosenbloom, K. Sims, et al., Imiglucerase (Cerezyme) improves quality of life in patients with skeletal manifestations of Gaucher disease, *Clin. Genet.* 71 (6) (2007) 576–588.
- [21] P. Kannus, J. Parkkari, H. Sievänen, A. Heinonen, I. Vuori, M. Järvinen, Epidemiology of hip fractures, *Bone*. 18 (1) (1996) S57–S63.
- [22] H. Mussawy, G. Ferrari, F.N. Schmidt, T. Schmidt, T. Rolvien, S. Hischke, et al., Changes in cortical microarchitecture are independent of areal bone mineral density in patients with fragility fractures, *Injury*. 48 (11) (2017) 2461–2465.
- [23] C.E. Kawalilak, J.D. Johnston, W.P. Olszynski, S.A. Kontulainen, Characterizing microarchitectural changes at the distal radius and tibia in postmenopausal women using HR-pQCT, *Osteoporos. Int.* 25 (8) (2014) 2057–2066.
- [24] J.E. Adams, Advances in bone imaging for osteoporosis. *Advances in bone imaging for osteoporosis*, *Nat. Rev. Endocrinol.* 9 (1) (2013) 28–42.
- [25] A. Kroker, R. Plett, K.K. Nishiyama, D.D. McErlain, C. Sandino, S.K. Boyd, Distal skeletal tibia assessed by HR-pQCT is highly correlated with femoral and lumbar vertebra failure loads, *J. Biomech.* 59 (2017) 43–49.
- [26] H.A. Fink, L. Langsetmo, T.N. Vo, E.S. Orwoll, J.T. Schousboe, K.E. Ensrud, et al., Association of High-resolution Peripheral Quantitative Computed Tomography (HR-pQCT) bone microarchitectural parameters with previous clinical fracture in older men: the osteoporotic fractures in men (MrOS) study, *Bone*. 113 (2018) 49–56.